NASA/TM—2002-211499

ASTROP2-LE: A Mistuned Aeroelastic Analysis System Based on a Two Dimensional Linearized Euler Solver

T.S.R. Reddy and R. Srivastava
University of Toledo, Toledo, Ohio

O. Mehmed
Glenn Research Center, Cleveland, Ohio

National Aeronautics and
Space Administration

Glenn Research Center

May 2002

Acknowledgments

This work was supported by a grant from the NASA Glenn Research Center, Structural Mechanics and Dynamics Branch under funding from the Advanced Subsonic Technology Project and the Turbomachinery and Combustion Technology Project. George Stefko, John Rohde, and Kestutis Civinskas are the program managers.

Available from

NASA Center for Aerospace Information
7121 Standard Drive
Hanover, MD 21076

National Technical Information Service
5285 Port Royal Road
Springfield, VA 22100

Available electronically at http://gltrs.grc.nasa.gov/GLTRS

ASTROP2-LE: A Mistuned Aeroelastic Analysis System based on a Two Dimensional Linearized Euler Solver

T.S.R. Reddy* and R. Srivastava*
The University of Toledo
Toledo, Ohio 43606

Oral Mehmed†
National Aeronautics and Space Administration
Glenn Research Center
Cleveland, Ohio 44135

Abstract

An aeroelastic analysis system for flutter and forced response analysis of turbomachines based on a two-dimensional linearized unsteady Euler solver has been developed. The ASTROP2 code, an aeroelastic stability analysis program for turbomachinery, was used as a basis for this development. The ASTROP2 code uses strip theory to couple a two dimensional aerodynamic model with a three dimensional structural model. The code was modified to include forced response capability. The formulation was also modified to include aeroelastic analysis with mistuning. A linearized unsteady Euler solver, LINFLX2D is added to model the unsteady aerodynamics in ASTROP2. By calculating the unsteady aerodynamic loads using LINFLX2D, it is possible to include the effects of transonic flow on flutter and forced response in the analysis. The stability is inferred from an eigenvalue analysis. The revised code, ASTROP2-LE for ASTROP2 code using Linearized Euler aerodynamics, is validated by comparing the predictions with those obtained using linear unsteady aerodynamic solutions.

Introduction

The aeroelastic research program at NASA Glenn Research Center is focused on flutter, and forced response analysis of turbomachinery. An overview of this research was presented in Ref. 1. The review showed that a range of aerodynamic and structural models have been used to obtain the aeroelastic equations. Both time and frequency domain methods have been used to obtain unsteady aerodynamic forces and to solve the aeroelastic equations. It was noted that time domain methods require large computational time compared to frequency domain methods, and should only be used when non-linearities are expected, and when the need justifies the cost.

Two approaches were used in obtaining the unsteady aerodynamic forces using frequency domain methods. In the first approach, Ref. 2, the unsteady aerodynamic equations are linearized about a uniform steady flow, there by neglecting the effects of airfoil shape, angle of attack and thickness. The unsteady aerodynamic models developed in Refs. 3-6 based on this approach are used in Refs. 7-8 to study the flutter and forced response analysis of a compressor rotor using a typical section structural model. Some of these models were also integrated with a

* Resident Research Associate, NASA Glenn Research Center, Cleveland, Ohio
† Research Engineer

three dimensional structural model using strip theory in Ref. 9. However, methods developed by this approach are restricted to shock-free flows and lightly loaded blade rows.

In the second approach, Ref. 10, the unsteady flow is regarded as a small amplitude perturbation about a non-uniform steady flow. The unsteady non-linear aerodynamic equations are linearized about the non-uniform steady flow, resulting in variable coefficient linear unsteady aerodynamic equations, which include the effects of steady aerodynamic loading due to airfoil shape, thickness and angle of attack. Following the second approach, Refs. 11-13 developed a nonlinear steady and linear unsteady aerodynamic model based on the potential equation. This unsteady aerodynamic model was used to study the effect of steady aerodynamic loading on flutter stability using a typical section structural model in Ref. 14. Subsequently this aerodynamic model was integrated with a three dimensional structural model using strip theory in Ref. 15.

However, the formulation based on the potential equation requires corrections for entropy and flow rotation. The Euler equations can be used to correctly model rotational and entropy effects associated with strong shocks. Unsteady linearized Euler aerodynamic models that include the effect of steady aerodynamic loading were developed in Refs. 16-18. Recently, a two dimensional linearized Euler code, LINFLX2D, was developed under a NASA contract and has been reported in reference 19. This code is based on the non-linear Euler solver developed in Ref. 20. The LINFLX2D code can be used with any aeroelastic code that uses a typical section aeroelastic model as its basis. In Ref. 21, the unsteady aerodynamic calculations from LINFLX2D were coupled with MISER (Ref. 7); a frequency domain aeroelastic stability and response code based on a typical section structural model. Flutter and forced response calculations were presented for cascades in subsonic and transonic flow, with and without mistuning.

The aeroelastic formulation in MISER does not represent the behavior of a three dimensional structure. An ideal analysis will be to couple a three dimensional structural analysis with a three dimensional aerodynamic analysis. This may be computationally intensive. An intermediate approach that couples a two dimensional aerodynamic analysis with a three dimensional structural model using strip theory, quasi-3D approach, may be less expensive computationally. This approach will provide accurate results except where three dimensional effects dominate. In turbomachines, where the compressors and turbines are enclosed, three dimensional effects may not be strong at least away from blade tip, and on stators, the strip theory can be used. The ASTROP2 code reported in Ref. 9 uses the strip theory approach for aeroelastic stability analysis.

The primary objective of the present study is to develop a quasi-3D aeroelastic code by coupling the 2-D linearized Euler analysis code, LINFLX2D, with a three dimensional structural model using strip theory. This effort uses the ASTROP2 code of Ref. 9 as the basis. The ASTROP2 code is a frequency domain stability analysis program, and as mentioned before uses strip theory to couple a two dimensional aerodynamic model with a three dimensional structural model. The present version of ASTROP2 has provision for flutter calculations, but not for forced response. During the course of the research effort, the ASTROP2 code is extended to include forced response calculation. Even though the formulation in ASTROP2 allowed for frequency mistuned cascade analysis, to the authors' knowledge, the code has never been validated and used for mistuned cascade analysis. In the present effort, the original formulation is modified to include both frequency mistuning and mode shape mistuning. The resulting code is named

ASTROP2-LE for ASTROP2 code using Linearized Euler aerodynamics, and validated by applying it to a representative blade. Brief descriptions of the formulation and method of analysis are given in the next section, followed by results and discussion.

Formulation

The aeroelastic formulation using the linearized approach requires solutions from two aerodynamic codes and a solution from a structural dynamic analysis code. The steady aerodynamic loads are obtained from a non-linear Euler solver, NPHASE, and the unsteady aerodynamic loads are obtained from LINFLX2D. The structural dynamic solution can be obtained from any finite element code, analytical solutions or measured data. The salient features of both the aerodynamic codes, and the aeroelastic formulation are described below.

Aerodynamic model

Non-linear Steady Euler Solver, NPHASE

The steady aerodynamic model is based on the unsteady, two-dimensional, Euler equations. The equations in conservative differential form are solved in a time-dependent body-fitted curvilinear reference frame. This transformation process and the ensuing numerical method are presented in detail in Ref. 20. The equations are discretized and solved using a finite volume method with a combination of flux difference splitting and flux vector splitting scheme. In addition, limiters are used to control dispersive errors commonly encountered with higher order schemes. The steady solutions presented herein are obtained using the implicit scheme developed in Ref. 20, which is third order accurate in space and second order accurate in time.

Linear Unsteady Euler Solver, LINFLX2D

To obtain the linearized unsteady Euler equations, the dependent variables in the unsteady non-linear Euler equations are expanded in an asymptotic series of the form

$$U = U(x) + u(x(x,t),t) + \quad \text{higher order terms} \tag{1}$$

where, the term U(x) is of order one and the second term is of the order ε. Substituting the expansion of Eq. 1 in the nonlinear unsteady Euler equations, and equating terms of like power in ε, and neglecting terms of second order in ε, nonlinear steady equations and linear variable coefficient unsteady equations are obtained. The unsteady linear equations are further simplified by assuming the unsteady excitations and responses are harmonic in time as

$$U = U(x) + \mathrm{Re}[u(x)\exp(i\,\omega t)] \tag{2}$$

For harmonic blade motions with constant phase angle between adjacent blades (interblade phase angle), the values of interblade phase angle (σ) that can occur are given as in Ref. 22.

$$\sigma_r = 2\pi r / N; \qquad r = 0,1,2,.....,N-1 \tag{3}$$

N is the number of blades in the cascade. In a time domain approach, the number of blocks required depends on the interblade phase angle, and small phase angles may require large number of blocks to calculate the unsteady aerodynamic forces. However, with the linear approach, the periodic conditions are applied on a single extended blade passage region i.e., a region of angular pitch,

$$\theta = 2\pi / N \tag{4}$$

In solving the linear unsteady equations, the independent variables are regarded as pseudo time dependent. This allows solutions to be determined using conventional time -marching algorithms to converge the steady and the complex amplitudes of the unsteady conservation variables to their steady state values. For more details, see reference 19.

Aeroelastic Model

As mentioned before, the ASTROP2 code of Ref. 9 is selected to couple the unsteady linearized aerodynamic solver, LINFLX2D. The ASTROP2 code uses strip theory to couple a two dimensional aerodynamic model with a three dimensional structural model. The present version of ASTROP2 can solve only for flutter and not for forced response. For clarity and completeness, the aeroelastic formulation in ASTROP2 is given here with extension to include forced response calculation.

ASTROP2 uses the normal mode approach for aeroelastic analysis. The equations of motion for the kth blade of the cascade for 'P' normal modes can be written as

$$[M]^k_{PxP}\{\ddot{\eta}\}^k_{Px1} + [\mathrm{K}]^k_{PxP}\{\eta\}^k_{Px1} = \{f_a^{\eta}\}^k_{Px1} + \{f_a\}^k_{Px1} \tag{5}$$

where $[\mathrm{M}]^k$ and $[\mathrm{K}]^k$ are generalized mass and stiffness matrices, $\{\eta\}^k$ is the generalized displacement vector, and $\left\{f^{\eta}{}_a\right\}^k$ is the motion dependent aerodynamic load vector, and $\left\{f_a\right\}^k$ is the motion independent aerodynamic load vector. The motion dependent forces cause flutter, and motion independent forces cause forced response (forced vibration). The elements of the matrices $[\mathrm{M}]^k$ and $[\mathrm{K}]^k$ are given by a free vibration analysis. The expressions for $\left\{f^{\eta}{}_a\right\}^k$ and $\left\{f_a\right\}^k$ using strip theory are given below. The expressions are developed in terms of the generalized displacement coordinates, $\{\eta\}$, (Ref. 23), instead of interblade phase angle modes as was done in Refs. 7 and 8.

In ASTROP2 the blades are divided into strips where the aerodynamic forces are calculated, see Fig. 1a. Each strip has two degrees of freedom, a plunging displacement, h, motion perpendicular to chord, and a pitching (torsion) displacement α, rotation about the leading edge of the strip (Fig. 1b). Using the normal modal values obtained from a free vibration analysis, the equivalent h and α for mth strip of the kth blade are given as summation of normal modes as

$$\{u_m\}^k = \begin{Bmatrix} h_m \\ \alpha_m \end{Bmatrix}_{2x1} = \begin{bmatrix} h_{m1} h_{m2} \cdots h_{mP} \\ \alpha_{m1} \alpha_{m2} \cdots \alpha_{mP} \end{bmatrix}_{2xP} \begin{Bmatrix} \eta_1 \\ \eta_2 \\ \vdots \\ \eta_P \end{Bmatrix}_{Px1} \tag{6.1}$$

or

$$\{u_m\}^k = [\phi_m]^k \{\eta\}^k \tag{6.2}$$

where $[\phi_m]$ is the modal matrix for the mth strip

It should be noted that when using ASTROP2, only the location of the strips has to be input to the code. ASTROP2 calculates the h and α values at these strips, and uses in the analysis i.e. the user need not input the h and α values at each strip for each mode.

Assembling for M strips, the modal matrix for the kth blade is given by

$$[\phi]^k = \begin{bmatrix} h_{11} h_{12} \cdots h_{1P} \\ \alpha_{11} \alpha_{12} \cdots \alpha_{1P} \\ \cdots\cdots\cdots\cdots \\ \cdots\cdots\cdots\cdots \\ h_{m1} h_{m2} \cdots h_{mP} \\ \alpha_{m1} \alpha_{m2} \cdots \alpha_{mP} \\ \cdots\cdots\cdots\cdots \\ \cdots\cdots\cdots\cdots \\ h_{M1} h_{M2} \cdots h_{MP} \\ \alpha_{M1} \alpha_{M2} \cdots \alpha_{MP} \end{bmatrix} \tag{6.3}$$

The motion dependent aerodynamic forces $\{f^{\eta}{}_a\}^k$ are given by

$$\{f_a^{\eta}\}^k = \omega^2 [\phi^k]^T_{Px2M} \{F\}^k_{2MxP} \tag{7}$$

where ω is the assumed frequency at which the aerodynamic forces are calculated, and $\{F\}^k$ is given as

$$\{F\}^k_{2MxP} = \sum_{n=1}^{N} [\psi]^{kn}_{2Mx2M} [\phi]^n_{2MxP} \{\eta\}^n_{Px1} \tag{8}$$

where N is the number of blades, and

$$[\psi]^{kn} = \begin{bmatrix} \begin{pmatrix} P_1^{kn} & Q_1^{kn} \\ R_1^{kn} & S_1^{kn} \end{pmatrix} & & & \\ & \ddots & & \\ & & \begin{pmatrix} P_m^{kn} & Q_m^{kn} \\ R_m^{kn} & S_m^{kn} \end{pmatrix} & \\ & & & \ddots \begin{pmatrix} P_M^{kn} & Q_M^{kn} \\ R_M^{kn} & S_M^{kn} \end{pmatrix} \end{bmatrix}_{2Mx2M} \tag{9}$$

with

$$P_m^{kn} = \frac{2\pi}{N} i\rho_m \frac{b_m^2}{k_m} l_m \sum_{r=1}^{N} (C_{Fq}^r) e^{i\frac{2\pi}{N} r(k-n)} \tag{10.1}$$

$$Q_m^{kn} = \frac{2\pi}{N} \rho_m \frac{b_m^3}{k_m^2} l_m \sum_{r=1}^{N} (C_{F\alpha}^r) e^{i\frac{2\pi}{N} r(k-n)} \tag{10.2}$$

$$R_m^{kn} = \frac{4\pi}{N} i\rho_m \frac{b_m^3}{k_m} l_m \sum_{r=1}^{N} (C_{Mq}^r) e^{i\frac{2\pi}{N} r(k-n)} \tag{10.3}$$

$$S_m^{kn} = \frac{4\pi}{N} \rho_m \frac{b_m^4}{k_m^2} l_m \sum_{r=1}^{N} (C_{M\alpha}^r) e^{i\frac{2\pi}{N} r(k-n)} \tag{10.4}$$

Here b_m, k_m, l_m, ρ_m are respectively the semichord, reduced frequency based on b_m, length of the strip, and air density at the mth strip. C_{Fq}^r and $C_{F\alpha}^r$ are the lift coefficients due to unit amplitudes of plunging and pitching displacements, and C_{Mq}^r and $C_{M\alpha}^r$ are the moment coefficients due to unit amplitudes of plunging and pitching displacements for the rth interblade phase angle, respectively.

The motion independent aerodynamic forces, $\{f_a\}^k$ are given by

$$\{f_a\}^k = \omega^2 \{G\}_{Px1}^k \tag{11}$$

where

$$\{G\}^k_{Px1} = [\phi^k]^T_{Px2M} \begin{Bmatrix} \{AD\}_1 \\ \{AD\}_2 \\ \vdots \\ \{AD\}_m \\ \vdots \\ \{AD\}_M \end{Bmatrix}^k_{2Mx1} \tag{12.1}$$

with

$$\{AD\}^k_m = \begin{Bmatrix} W1^k_m \\ W2^k_m \end{Bmatrix}_{2x1} \tag{12.2}$$

$$W1^k_m = -2\pi\rho_m \frac{b_m^3}{k_m^2} \sum_{r=1}^{N} \frac{w_r}{U} C^r_{Fw} e^{i\frac{2\pi r}{N}k} \tag{12.3}$$

$$W2^k_m = -4\pi\rho_m \frac{b_m^4}{k_m^2} \sum_{r=1}^{N} \frac{w_r}{U} C^r_{Fw} e^{i\frac{2\pi r}{N}k} \tag{12.4}$$

Here C^r_{Fw} and C^r_{Mw} are the lift and moment coefficients due to unit amplitudes of the wake, and w_r is the amplitude of the velocity of the sinusoidal wake in the r^{th} interblade phase angle mode. Since the forced response problem is typically for a given interblade phase angle, σ (r = R), Eq. 12.3 and 12.4 can be written as

$$W1^k_m = -2\pi\rho_m \frac{b_m^3}{k_m^2} \frac{w_R}{U} C^R_{Fw} e^{i\frac{2\pi R}{N}k} \tag{12.5}$$

$$W1^k_m = -4\pi\rho_m \frac{b_m^4}{k_m^2} \frac{w_R}{U} C^R_{Mw} e^{i\frac{2\pi R}{N}k} \tag{12.6}$$

For the present analysis, the aerodynamic force coefficients in Eq. 10 and Eq. 12 are obtained using the linear unsteady aerodynamic model of Ref. 3 and the LNFLX2D of Ref. 19.

Substituting Eq. 7 and Eq. 11 in Eq. 5, equation 5 can be written as

$$[M]^k\{\ddot{\eta}\}^k + [K]^k\{\eta\}^k = \omega^2 \sum_{n=1}^{N} [A]^{kn}\{\eta\}^n + \omega^2\{G\}^k \tag{13}$$

where

$$[A]^{kn}_{PxP} = [\phi^k]^T_{Px2M} [\psi]^{kn}_{2Mx2M} [\phi^n]_{2MxP} \tag{14}$$

It should be noted that Eq. 14 permits the use of mode shapes that differ from blade to blade.

By writing the above equation for all blades, the equations of motion for the cascade can be written as

$$[M_g]\{\ddot{X}\}+[K_g]\{X\}=\omega^2[A]\{X\}+\omega^2\{G\} \tag{15}$$

where

$$[M_g]=\begin{bmatrix}[M]^1 & & \\ & [M]^2 & \\ & & \ddots[M]^N\end{bmatrix}_{NPxNP} \tag{16.1}$$

$$[K_g]=\begin{bmatrix}[K]^1 & & \\ & [K]^2 & \\ & & \ddots[K]^N\end{bmatrix}_{NPxNP} \tag{16.2}$$

$$[A]=\begin{bmatrix}[A]^{11}\,[A]^{12}\cdots[A]^{1N} \\ [A]^{21}\,[A]^{22}\cdots[A]^{2N} \\ \vdots \qquad\qquad \vdots \\ [A]^{N1}\,[A]^{N2}\cdots[A]^{NN}\end{bmatrix}_{NPxNP} \tag{16.3}$$

$$\{G\}=\begin{Bmatrix}\{G\}^1 \\ \{G\}^2 \\ \vdots \\ \{G\}^N\end{Bmatrix}_{NPx1} \tag{16.4}$$

$$\{X\} = \begin{Bmatrix} \begin{Bmatrix} \eta_1 \\ \eta_2 \\ \vdots \\ \eta_P \end{Bmatrix}^1 \\ \begin{Bmatrix} \eta_1 \\ \eta_2 \\ \vdots \\ \eta_P \end{Bmatrix}^2 \\ \vdots \\ \begin{Bmatrix} \eta_1 \\ \eta_2 \\ \vdots \\ \eta_P \end{Bmatrix}^N \end{Bmatrix}_{NPx1} \tag{16.5}$$

The individual blade matrices, $[M]^k$ is of size PxP, and consists of the mass matrix of the k^{th} blade, with elements given as

$$M_{ii} = m_i,\ i = 1,P \tag{17.1}$$

where m_i is the i^{th} modal mass. Similarly, $[K]^k$ is of size PxP, and consists of the stiffness matrix of the k^{th} blade, with elements given as

$$K_{ii} = M_{ii} * \omega_i^2 (1 + 2i\varsigma_i),\ i = 1,P \tag{17.2}$$

where ω_i is the natural frequency of the i^{th} mode and ς_i is structural damping ratio of the i^{th} mode.

Each element of $[A]^{kn}$ and $\{G\}^k$ are given by summing over M strips as

$$A^{kn}{}_{ij} = \sum_{m=1}^{M} (h_{mi}\alpha_{mi})^k \begin{bmatrix} P^{kn}{}_m & Q^{kn}{}_m \\ R^{kn}{}_m & S^{kn}{}_m \end{bmatrix} \begin{Bmatrix} h_{mj} \\ \alpha_{mj} \end{Bmatrix}^n \tag{18.1}$$

$$G_i^k = \sum_{m=1}^{M} (h_{mi}\ \alpha_{mi})^k \begin{Bmatrix} W1_m \\ W2_m \end{Bmatrix}^k \tag{18.2}$$

Assuming the solution for Eq. 15 is of the form

$$\{X\} = \{\overline{X}\} e^{i\omega t} \tag{19}$$

and dividing both sides by an assumed frequency, ω_0^2, and rearranging, the Eq. 15 can be written as:

$$[[P]-\gamma[Q]]\{\bar{X}\}=\gamma\{G\} \tag{20}$$

where

$$[P]=\frac{1}{\omega_0^2}[K_g] \tag{21.1}$$

$$[Q]=[M_g]+[A] \tag{21.2}$$

For a stability calculation (flutter), the motion-independent forces {G} are set to zero and the eigenvalue problem is obtained in the standard form:

$$[[P]-\gamma[Q]]\{\bar{X}\}=\{0\} \tag{22}$$

The solution of the above eigenvalue problem (22) results in NP complex eigenvalues of the form

$$i\left(\frac{\omega}{\omega_0}\right)=i\sqrt{\gamma}=\mu+i\nu \tag{23}$$

The real part of the eigenvalue (μ) represents the damping ratio, and the imaginary part (ν) represents the damped frequency; flutter occurs if $\mu \geq 0$ for any of the eigenvalues.

The aeroelastic response of the blades induced by wakes is calculated from equation (20) as

$$\{\bar{X}\}=[[P]-\gamma[Q]]^{-1}\gamma\{G\} \tag{24}$$

tuned cascade

For a tuned cascade, in which all the blades have identical structural properties, the interblade phase angle modes are uncoupled. The equation of motion can be solved for each interblade phase angle, σ_R for the R^{th} mode, given by Eq. 3. For tuned cascade analysis, Eq, 13 can be written as

$$[M]^k\{\ddot{\eta}\}^k+[K]^k\{\eta\}^k=\omega^2[A]^R\{\eta\}+\omega^2\{G\}^R \tag{25}$$

Since the blades are identical, the same equation is obtained for each blade, and superscript 'k' can be dropped. The unsteady aerodynamic force coefficients in calculating [A], Eq. 10, are given by

$$P_m = 2\pi i \rho_m \frac{b_m^2}{k_m} l_m C_{Fq}^R \tag{26.1}$$

$$Q_m = 2\pi \rho_m \frac{b_m^3}{k_m^2} l_m C_{F\alpha}^R \tag{26.2}$$

$$R_m = 4\pi i \rho_m \frac{b_m^3}{k_m} l_m C_{Mq}^R \tag{26.3}$$

$$S_m = 4\pi \rho_m \frac{b_m^4}{k_m^2} l_m C_{M\alpha}^R \tag{26.4}$$

$$W1_m = -2\pi \rho_m \frac{b_m^3}{k_m^2} \frac{w_R}{U} C_{Fw}^R \tag{26.5}$$

$$W2_m = -4\pi \rho_m \frac{b_m^4}{k_m^2} \frac{w_R}{U} C_{Mw}^R \tag{26.6}$$

Equation 25 is solved for N different values of the interblade phase angle given by Eq. 3. It is to be noted here that the size of the matrices for solution is now reduced to PxP compared to (NPxNP) for mistuned case. As before, the equations for the stability (flutter) problem are obtained by setting the motion-independent forces to zero. For a given interblade phase angle, the solution of the eigenvalue problem results in P complex eigenvalues of the form given by Eq. 23 and flutter occurs if $\mu \geq 0$ for any of the eigenvalues. The eigenvalue problem is solved for each of the N permissible values. The critical phase angle is identified as the one that results in the lowest flutter speed.

Stability calculation

The aerodynamic coefficients have to be calculated before the eigenvalue problem can be set up and solved. Since the unsteady aerodynamic coefficients depend on the frequency of oscillation, it is necessary to assume a frequency ω_0 (actual input to the code may be the reduced frequency of blade vibration based on chord, $k_c = \omega c / U$, where U is the free stream velocity) in advance to be able to calculate the aerodynamic coefficients. The aerodynamic coefficients are functions of inlet Mach number M, and interblade phase angle σ_r, in addition to cascade geometric parameters. In the present study, for a given inlet Mach number, the reduced frequency is varied until the real part of one of the eigenvalues μ becomes zero while the real parts of the remaining eigenvalues are negative. This is repeated for all possible interblade phase angles for a tuned cascade. The assumed flutter-reduced frequency k_{cf} and the calculated flutter frequency ν_f are both based on ω_f. Thus, these two can be combined to eliminate ω_f and the flutter speed is obtained, namely, $U_f = \nu_f c \omega_0 / k_{cf}$. Since the inlet Mach number is known, this flutter speed gives the inlet condition (speed of sound, a_∞) at which the cascade will be neutrally stable for

the given Mach number. This procedure can be repeated to obtain a plot of flutter speed versus Mach number. Knowing the operating conditions, it is possible to determine whether flutter will occur within the operating region and if so, the Mach number and frequency at flutter. It should be noted that a mistuned cascade can also be analyzed using this procedure but will require the solution of the equations for all phase angles at one time for a given reduced frequency.

Analysis procedure

The flutter and forced response analysis in FREPS-LE consists of running five codes, (I) a structural dynamic analysis code, such as NASTRAN, ANSYS, etc., (II) 2DSTRIP, (III) NPHASE, (IV) LINFLX2D, and (V) 2DASTROP. It is to be noted that ASTROP2 code is a combination of 2DSTRIP and 2DASTROP codes. The analysis procedure is explained in five steps. In step 1 a vibration analysis is performed for the blade. The output is natural frequencies and mode shapes. This output is used by the 2DSTRIP code. In step 2, strips are selected, and 2DSTRIP is run to calculate relative Mach numbers, sweep angles, stagger angles, chord values, and strip widths at these strips. During this run, the three dimensional modal values are also interpolated at each strip, and equivalent pitching and plunging modal values are calculated. In step 3, a steady aerodynamic solution at these strips is obtained from NPHASE. The steady aerodynamic solution is written as a database. Step 4 consists of running LINFLX2D for assumed number of reduced frequencies, interblade phase angles, for pitching and plunging modes. The analysis is carried out for unit amplitude of vibration for all the strips, and the unsteady aerodynamic solutions are stored as a database. In step 5, the 2DASTROP code is executed to calculate flutter using the eigenvalue approach and to calculate forced response. The number of calculations required for the aeroelastic analysis depend on the number of strips, Mach numbers, interblade phase angles, and reduced frequencies as described below.

Let each blade be divided into NSTRIP number of strips. In general, for a given inlet Mach number, the flow conditions, (relative Mach number and angle of attack), and the geometric conditions, (gap to chord ratio, stagger angle, and airfoil shape) will be different at these strips. Therefore, the number of steady aerodynamic solutions (number of NPHASE runs) required is NSTDY = NMACH * NSTRIP, where NMACH is the number of inlet Mach numbers to be considered in the study.

In the case of the unsteady aerodynamic solution, three other parameters, number of modes, reduced frequency (k_c) and interblade phase angle (σ) have to be considered. If NMODE is the number of modes, NREDF is the number of reduced frequencies, and NSIGMA is the number of interblade phase angles, then the number of unsteady solutions for flutter (number of LINFLX2D runs) is, NUSTDY = NSTRIP*NMACH *NMODE *NSIGMA *NREDF. It is to be noted that NSIGMA is equal to the number of blades of the cascade. The forced response is usually calculated for a specific excitation at a fixed interblade phase angle and at a given frequency. Therefore, the number of unsteady runs for forced response are reduced to NUSTDY = NSTRIP*NMACH, same as for steady solution.

The main purpose of the present effort is to couple the unsteady aerodynamic solutions from LINFLX2D to ASTROP2 code and to validate the procedure. In order to reduce the number of calculations required for the aeroelastic analysis, a straight, untapered stator blade at two inlet Mach numbers will be considered for the present study. Therefore, for each Mach number, the flow and geometric conditions will be same at all strips, reducing the number of steady

aerodynamic calculations to NMACH, i.e. NSTDY = 2. For the unsteady run, the number of modes is fixed as two, plunging and pitching, i.e. NMODE=2. The number of unsteady runs for flutter is given as NUSTDY = 2 *2 *NSIGMA *NREDF = 4*NSIGMA* NREDF. For predicting the flutter boundary, calculations have to be carried out for a number of reduced frequencies. It is suggested that a LINFLX2D database be prepared for three or four reduced frequencies, and then interpolation be used for required frequencies. These reduced frequency values can be selected by first running ASTROP2-LE with linear theory. The number of unsteady runs for forced response is given by NUSTDY =2.

Results and Discussion

Results presented here are meant to demonstrate the state of development of the code and to show that the analysis procedure given in the previous sections has been implemented correctly. Therefore, calculations are made for a non-rotating cantilevered blade, representing a stator blade of a turbomachinery component. Results are presented for an assembly of 12 blades on a rigid disk coupled only aerodynamically. Similar geometry is also considered in Ref. 23.

Both tuned and mistuned cascade analyses are carried out for a flat plate and the tenth standard configuration, (designated as C10, Ref. 19) airfoil cross sections. A 20% alternate mistuning is considered for the mistuning analysis. The gap to chord ratio (s/c) is 1.0 and the stagger angle (theta) is 45 degrees. Two inlet Mach numbers are considered M=0.7 and 0.8. For the C10 airfoil and for M=0.8, the flow is transonic with a shock near the quarter chord. An H-grid of 141x41 grid is used for the study. There are 80 points on the airfoil, and the inlet boundary is 5 chords from the airfoil leading edge and the exit boundary is 10 chords from the airfoil trailing edge. Steady aerodynamic solutions were obtained for these Mach numbers using NPHASE before running LINFLX2D.

LINFLX2D code:

To validate the LINFLX2D code, unsteady aerodynamic pressure differences were calculated for both airfoil cross sections for a reduced frequency of oscillation based on chord (k_c) of 1.0. The unsteady pressure difference is non-dimensionalized by (upper surface pressure- lower surface pressure)/(airdensity*U**2*amplitude of oscillation).

Subsonic Inflow

Figure 2a shows the steady Mach number distribution obtained for the C10 airfoil cascade for an inlet Mach number, M=0.7. The flow to the cascade is at 10 degrees angle of attack. It can be seen that for this Mach number the flow is shock free. The unsteady pressure difference distribution for an interblade phase angle, σ, of 180 degrees is shown in Fig. 2b. The blades are oscillating in pitch about the midchord. Figure 2b shows predictions from linear theory (Ref. 4) and from the linearized Euler code LINFLX2D for flat plate geometry, from the nonlinear Euler (Ref. 17) and from LINFLX2D for the C10 airfoil geometry. The unsteady pressure difference distribution obtained with LINFLX2D for the flat plate geometry correlates very well with linear theory. Also, the predictions from LINFLX2D for the C10 geometry correlate well with the nonlinear Euler results indicating that the unsteady aerodynamic pressures predicted by

LINFLX2D are accurate. From this figure the effect of geometry, angle of attack and blade thickness can also be seen indicating the importance of including these features in the unsteady aerodynamic analysis.

Transonic Inflow

For the C10 airfoil cascade geometry, and for an inlet Mach number of 0.8, the flow is transonic with a normal shock occurring in each blade passage. The steady Mach number distribution obtained from NPHASE is shown in Fig. 3a for a steady angle of attack of 13 degrees. A normal shock occurs on the suction surface at about 28% of the chord. Results from the full potential solver, Ref. 12, are also included for comparison. Both results agree well, except that the nonlinear steady Euler solver, NPHASE, predicts the shock location slightly downstream of that predicted by the full potential solver of Ref. 12. A shock fitting procedure was used in Ref. 12, whereas the shock is captured naturally in the present solver.

The unsteady pressure distribution is shown in Fig. 3b, along with a comparison with linear theory (Ref. 4) and the unsteady nonlinear Euler solver. The unsteady results are for pitching about mid-chord with $k_c = 1.0$, $\sigma = 180°$ and amplitude of oscillation, $\alpha_0, = 2°$. As expected, linear theory does not show any shock, indicating that unsteady analysis based on linear theory will not be accurate for cascade flutter analysis in transonic flow. A fair correlation between LINFLX2D and non-linear unsteady Euler results can be seen in Fig. 3b. The differences could be due to the fact that for transonic flow the following factors may have more effect than for in subsonic flow: (1) grids used or (2) the steady solution on which LINFLX2D based is not a low loss solution, which is a requirement for an accurate solution from LINFLX2D. These issues need separate study.

Similar results were obtained for plunging motion for both subsonic and transonic inflows.

ASTROP2 code

The ASTROP2 code was validated for flutter prediction in Ref. 9 by calculating the flutter boundary of the SR3CX2 advanced propeller. The vibration characteristics of the propeller blade were obtained from the finite element structural analysis code NASATRAN. Linear theory of Ref. 5 was used for calculating the unsteady aerodynamic forces. For more details on the ASTROP2 code, see references 9, 24 and 25. In the present effort, forced response capability was added to the ASTROP2 code, and modifications were made for the analysis of mistuned cascades. To validate these upgrades, the calculations from ASTROP2 were compared with those obtained from MISER code, Ref. 7 in appendix A. The validation was done for both flutter and forced response. As can be seen from the results shown in appendix A, the results from the current version of ASTROP2 agree well with those obtained from MISER.

Aeroelastic Calculations

A 12 blade stator is considered for stability and response calculations. In general, the procedure for aeroelastic analysis starts with a database of the stator blade containing the geometry, mode shapes, and modal frequencies. Then strips are selected, and 2DSTRIP is run to calculate the relative Mach numbers, sweep angles, stagger angles, chord values, and strip widths at these

strips. During this run, the three dimensional modal values are interpolated at each strip, and equivalent pitching and plunging modal values are obtained. Then the steady and unsteady aerodynamic solutions are obtained for these strips, and used for flutter and response analysis.

However, the main aim of this paper is to demonstrate the ASTROP2 and LINFLX2D code coupling. Therefore, the analysis is carried out for the simplified geometry of straight, untwisted stator blades. Mode shapes, frequencies, and modal values are *assumed* instead of performing a detailed analysis. Two assumed modes are used in the analysis. The first mode is a pure torsion mode and the second mode is a coupled bending-torsion mode. The natural vibration frequencies are 81.376HZ and 148.02 HZ respectively. The blade is divided into 10 strips. Table 1 shows the aerodynamic and geometric input parameters at the 10 strips. With identical flow and geometric conditions, the only contribution to the generalized aerodynamic force matrix at the strip is due to the different modal values at each strip. Table 2 shows the modal values used in this study.

The unsteady force coefficients are calculated using LINFLX2D for harmonic blade vibration in plunging and pitching modes for a reduced frequency, k_c, of 0.2 based on chord. The reduced frequency used to calculate the unsteady aerodynamic coefficients, k_c=0.2 corresponds to a frequency of 96.07 HZ. The same grids that were used for the unsteady validation and the NPHASE steady solution obtained in the previous section were used again. The moment coefficients are calculated about the leading edge. The calculated unsteady force coefficients along with the modal values at the strips are used by 2DASTROP code to calculate the elements of [A] and {G}. The stability is inferred from the eigenvalues.

Stability calculations

Figure 4 shows the root locus plot of the eigenvalues for mode 1 calculated for flat plate geometry operating at M=0.7. Results obtained from LINFLX2D are compared with those obtained using linear theory unsteady aerodynamics. Good correlation is observed. At M=0.7 the flow field is linear hence, linear theory and linearized Euler are expected to correlate well with each other. The linear theory unsteady aerodynamic code was an integral part of ASTROP2, and LINFLX2D is the new code that is coupled with ASTROP2. The root locus plot correlation shows that the coupling of the LINFLX2D unsteady aerodynamic database to ASTROP2 is accurate. It is to be noted that since the first mode is a pure torsional mode, the frequency of the aeroelastic system is close to the first natural frequency of the blade.

To explore the effects of airfoil shape, and transonic flow the analysis was carried out with the C10 geometry and for M=0.7 and 0.8. Figure 5a shows the root locus plot for a tuned cascade for the first mode at an inflow M of 0.7 for the flat plate and C10 airfoil geometries. For the tuned case, it can be seen that the blade is more unstable when the effect of airfoil geometry is included. The root locus plot for the first mode for tuned cascade for M=0.8 is shown in Fig. 5b. Here the root locus plot shows the effect of airfoil shape, and transonic flow. It is seen that the tuned blade is slightly less unstable than in figure 5a when the effects of airfoil geometry, and shock are included.

To include the effect of mistuning, the first mode frequency of the alternate blades is increased/decreased by 20% i.e. two adjacent blades have frequency of 1.1 f1 and 0.9 f1, where

f1 is the tuned first mode frequency. The root locus plot for the tuned and mistuned rotors is shown in figure 6. The frequencies are plotted on double Y -axis; left Y -axis representing tuned cascade frequencies (circles), and right Y-axis representing mistuned cascade frequencies (triangles). The open symbols represent flat plate airfoil, and closed symbols represent C10 airfoil.

Figure 6a shows the root locus plot for mistuned cascade for the first mode at an inflow M of 0.7 for the flat plate and C10 airfoil geometries. For comparison, the root locus plot of the tuned cascade is also shown in Fig. 6a. It can be seen that the mistuning increased the spread of the blade frequencies for both geometries. It can also be seen that (1) root locus plot has split into two parts, one corresponding to high frequency, and the other to low frequency, (2) the rotor with the flat plate geometry became stable with the addition of mistuning, (3) the rotor with the C10 airfoil geometry also moved towards the stable direction, but the amount of mistuning was not sufficient to make the rotor stable.

The root locus plot for the first mode for M=0.8 for the mistuned cascade is shown in Fig. 6b. Here the root locus plot shows the effect of airfoil shape, transonic flow and mistuning. The effect of mistuning is same as that for M = 0.7.

Response Calculations

The response of the blade to a vortical disturbance is calculated for flat plate geometry and compared with that obtained from linear theory. A structural damping ratio of 0.002 is added to make the aeroelastic system stable (see Fig. 4 – 6) and to limit the amplitude at resonance. Figure 7 shows the tuned aeroelastic response for R=6 i.e. σ =180 degrees for flat plate geometry. The unsteady aerodynamic coefficients are obtained at $k_C = 0.2$ for M=0.7. The moment coefficients are calculated about the leading edge. The forcing frequency range investigated is limited to a small range around the 1st mode frequency. For the tuned cascade, the response will be entirely in the r = R mode, and all the blades will have equal amplitudes. The amplitude of response is a function of the frequency ratio, ω / ω_o. Figure 7 shows the 1st generalized degree of freedom (q1) response obtained using linear theory (Ref. 5) and present LINFLX2D code. It can be seen that calculations from linear theory and from LINFLX2D are identical indicating that the coupling of LINFLX2D coefficients to ASTROP2 code for response calculations is accurate.

Figure 8 shows the q1 response obtained for the C10 airfoil for M=0.7. Comparing the response of C10 with that of flat plate, it can be seen that the response has increased about 140%. This is due to high steady loading on the airfoil. Figure 8 also shows the response with 20% alternate mistuning for both flat plate geometry and C10 geometry. The response has split into two resonance peaks, one for odd blades and one for even blades with equal amplitude, and same as that without mistuning. This indicates that the effect of aerodynamic damping is very small for the example chosen here.

Figure 9 shows the q1 response obtained for the C10 airfoil for M=0.8. Comparing the response of C10 with that of flat plate, it can be seen that the response has increased to only about 68%. Observing from Fig 8 that the airfoil shape increased the response to about 140%, the decrease in the response in Fig 9 can be attributed to the presence of shock. However, the flow being

transonic, it is necessary to check the present calculation by running LINFLX2D for a different grid. Figure 9 also shows the response calculations with 20% alternate mistuning. Again, the response has split into two resonance peaks, on for odd blades and one for even blades with equal amplitude, and same as that without mistuning. This again indicates that the effect of aerodynamic damping is very small for the example chosen here.

The response calculations given above were carried out by including the motion dependent aerodynamic matrix, [A], which adds the contribution of aerodynamic damping to the response. For the case considered here, the calculations were repeated without the contributions of [A]. The response showed negligible change in the amplitude. This may be due to low aerodynamic damping contribution from [A] (see Figs. 4-6) compared to the added structural damping ratio of 0.002. Note that the calculation of the elements of [A] requires calculation of aerodynamic coefficients for all interblade phase angles (equal to the number of blades) where as calculation of the elements of {G} requires the aerodynamic forcing coefficient for only one phase angle.

Computational times

The unsteady aerodynamic solution times varied from 20 minutes to 75 minutes on an SGI workstation. This is directly related to the number of iterations required for convergence. A solution for flat plate geometry took more time than for the C10 airfoil geometry.

Concluding Remarks

The transonic flow unsteady linearized Euler aerodynamic solver, LINFLX2D, has been successfully coupled with the ASTROP2 aeroelastic analysis code. The resulting code, ASTROP2-LE, is validated by comparing predictions from linear theory for flat plate geometry. Comparison was done for both flutter and forced response. Results were also presented for cascades in subsonic and transonic flow for a standard cascade section known as C10 geometry. In addition the code is validated by comparing results for MISER code. It is noted that the number of LINFLX2D solutions required is directly related to number of strips. Care has to be taken in selecting the number of strips to reduce the number of calculations. The following were observed during the study: (1) The steady loading due to the airfoil shape and angle of attack destabilized the cascade for the Mach numbers considered, (2) The steady loading due to the airfoil shape and angle of attack increased the blade response for subsonic flow and decreased response for transonic flow compared to that for a flat plate, (3) for the cascade geometry considered here, even 20% mistuning has very small effect on flutter and negligible effect on response.

APPENDIX A

Comparison of ASTROP2-LE calculations with MISER

In the present research effort, forced response capability was added to the ASTROP2-LE code, and modifications were made for the analysis of mistuned cascades. To validate these upgrades, the calculations from ASTROP2-LE were compared in this appendix with those obtained from MISER code, Ref. 8. The validation was carried out for both flutter and forced response.

A uniform blade is considered with a chord of 2.0 units and a span of 1.0 unit. Since the main aim is to validate the calculation of the aerodynamic matrices, the mass and stiffness matrices were taken from MISER, and used in ASTROP2-LE. Two modes are used in the calculations, with first mode as {h,alfa) = (1.0,0.0) and the second mode as {h, alfa) = (0.0, 1.0) at all strips. The Mach number is 0.7. The gap to chord ratio is 1.0 and the stagger angle is 45 degrees. The linear theory of Ref. 5 is used to calculate the elements of the aerodynamic matrices. Table A.1 shows the elements of the mass and stiffness matrices.

Table A.2 shows the comparison of the elements of the aerodynamic and force matrices, stability, and response predictions for a tuned cascade. A reduced frequency of 0.5 based on semichord is (k_b) used. The interblade phase angle is 180.0 degrees. The blades are oscillating about the leading edge. The table shows results from ASTROP2-LE and from MISER code. As seen from table A.2, the ASTROP2-LE calculations compare very well with those of MISER, validating the ASTROP2-LE modifications for flutter and forced response of tuned cascades.

To validate the code for mistuned cascade analysis, a 12 blade cascade is considered. The blades are assumed to have alternate frequency mistuning of 20% in second mode i.e. the frequency of every alternate blade is 0.9f1 and 1.1f1 where f1 is tuned blade frequency of the second mode.

Figure A1 shows the root locus plot, real part of the eigenvalue versus imaginary part of the eigenvalue, for 12 bladed cascade with and without mistuning. Second mode is plotted. The reduced frequency k_b is 0.5, and the blades are pitching about the leading edge. As can be seen ASTROP2 predictions compare exactly with MISER calculations.

Figure A2 shows the amplitude of the second mode plotted with varying frequency ratio. A structural damping ratio of 0.002 was used to limit the amplitude of the blades at resonance. The interblade phase angle of the forcing function is 180 degrees corresponding to an engine order excitation of 6. The reduced frequency k_b is 0.5, and the blades are pitching about the leading edge. Again, it can be seen that the prediction from ASTROP2 match exactly with MISER calculations.

This validates the ASTROP2 code and the modifications.

References

(1) Reddy, et al, "A review of Recent Aeroelastic Analysis Methods for Propulsion at NASA Lewis Research Center," NASA TP–3406, December 1993.

(2) Whitehead, D.S., "Classical Two-Dimensional Methods," Chapter II in AGARD Manual on Aeroelasticity in Axial Flow in Turbomachines, Vol. 1, Unsteady Turbomachinery Aerodynamics, (ed. M.F. Platzer and F.O. Carta), AGARD–AG–298, Mar. 1987.

(3) Whitehead, D.S., "Force and Moment Coefficients for Vibrating Airfoils in Cascades," Aeronautical Research Council R&M 3254, Feb. 1960.

(4) Smith, S.N., "Discrete Frequency Sound Generation in Axial Flow Turbomachines," British Aeronautical Research Council, London, ARC R&M No. 3709, 1971.

(5) Rao, B.M. and Jones, W.P., "Unsteady Airloads on a Cascade of Staggered Blades in Subsonic Flow," Paper No. 32, AGARD–CP–177, September 1975.

(6) Adamczyk, J.J. and Goldstein, M.E., "Unsteady Flow in a Supersonic Cascade with Subsonic Leading-Edge Locus," ***AIAA Journal***, Vol. 16, No.12, pp. 1248–1254, Dec. 1978.

(7) Kaza, K.R.V. and Kielb, R.E., "Flutter and Response of a Mistuned Cascade in Incompressible Flow," ***AIAA Journal***, Vol. 20, No. 8, pp. 1120–1127, 1982.

(8) Kielb, R.E. and Kaza, K.R.V., "Aeroelastic Characteristics of a Cascade of Mistuned Blades in Subsonic and Supersonic Flows," ***ASME Journal of Vibration, Acoustics, Stress and Reliability of Design***, Vol. 105, pp. 425–433, Oct. 1983.

(9) Kaza, K.R.V., Mehmed, O., Narayanan, G.V., and Murthy, D.V., "Analytical Flutter Investigation of a Composite Propfan Model," ***Journal of Aircraft***, Vol. 26, No. 8, Aug. 1989, pp. 772–780.

(10) Verdon, J.M., "Linearized Unsteady Aerodynamic Theory," Chapter II in AGARD Manual on Aeroelasticity in Axial Flow in Turbomachines, Vol. 1, Unsteady Turbomachinery Aerodynamics, (ed. M.F. Platzer and F.O. Carta), AGARD–AG–298, Mar. 1987.

(11) Verdon, J.M. and Caspar, J.R., "Development of a Linear Unsteady Aerodynamic Analysis for Finite Deflection Subsonic Cascades," ***AIAA Journal***, Vol. 20, pp. 1259–1267, 1982.

(12) Verdon, J.M. and Caspar, J.R., "A Linearized Unsteady Aerodynamic Analysis for Transonic Cascades," ***Journal of Fluid Mechanics***, Vol. 149, pp. 403–429, 1984.

(13) Hoyniak, D., Verdon, J.V., "Steady and Linearized Unsteady Transonic Analyses of Turbomachinery Blade Rows," Unsteady Aerodynamics and Aeroelasticity of Turbomachines, Y. Tanida and M. Namba (editors), pp. 109–124, 1995.

(14) Smith, T.E. and Kadambi, J.R., "The Effect of Steady Aerodynamic loading on the Flutter Stability of Turbomachinery Blading," ***Journal of Turbomachinery***, Vol. 115, No. 1, pp. 167–174, 1993.

(15) Smith, T.E., "A Modal Aeroelastic Analysis Scheme for Turbomachinery Blading," NASA CR 187089, March 1991.

(16) Hall, K.C. and Clark, W.S., "Linearized Euler Predictions of Unsteady Aerodynamic Loads in Cascades," ***AIAA Journal***, vol. 31, No. 3, pp. 540–550, March 1993.

(17) Holmes, D.G. and Chuang, H.A., "2D Linearized Harmonic Euler Flow Analysis for Flutter and Forced Response," Unsteady Aerodynamic, Aeroacoustics, and Aeroelasticity of Turbomachines and Propellers, pp. 213–230, Ed. Atassi, H.M, Springer-Verlag, New York, 1993

(18) Kahl, G. and Klose, A., "Computation of Time Linearized Transonic Flow in Oscillating Cascades," ASME Paper 93–GT–269, 38th IGT and Aeroengine Congress and Exposition, Cincinnati, Ohio, May 24–27, 1993.

(19) Verdon, J.V., Montgomery, M.D. and Kousen, K.A.," Development of a Linearized Unsteady Euler Analysis for Turbomachinery Blade Rows," NASA CR–4677, June 1995.

(20) Swafford, T.W., et al, "The Evolution of NPHASE: Euler/ Navier-Stokes Computations of Unsteady Two Dimensional Cascade Flow Fields," AIAA Paper 94–1834, 12th Applied Aerodynamics Conference, Colorado Springs, Colorado, June 20–23, 1994

(21) Reddy, T.S.R., Srivastava, R. and Mehmed, O., "Flutter and Forced Response Analysis of Cascades Using a Two Dimensional Linearized Euler Solver," NASA/TM—1999-209633, November 1999, Part of the material is presented as AIAA–98–3433, 34th Joint Propulsion Conference & Exhibit, July 13–15, 1998, Cleveland, OH.

(22) Lane, F., "System Mode Shapes in the Flutter of Compressor Blade Rows, ***Journal of the Aeronautical Sciences***, Vol. 23, pp. 54–66, Jan. 1956.

(23) Srinivasan, A.V. and Fabunmi, J.A., "Cascade Flutter Analysis of Cantilevered Blades," Transactions of the ASME, **Journal of Engineering for Gas Turbines and Power**, Vol. 106, pp. 34–43, January 1984.

(24) Narayanan, G.V. and Kaza, K.R.V., ASTROP2 Users Manual: A Program for Aeroelastic Stability Analysis of Propfans, Version 1.0, NASA TM–4304, August 1991.

(25) Reddy, T.S.R. and Lucero, J.M., ASTROP2 Users Manual: A Program for Aeroelastic Stability Analysis of Propfans, Version 2.0, NASA TM–107195, March 1996.

Table 1: Aerodynamic Input Parameters at the Strips

Atmospheric pressure (psi)=13.1023; Speed of sound (fps)=1130.0

Strip Index	Stagger Angle (Degrees)	Chord Length (Inches)	Gap/Chord Ratio	Radius (Inches)	Strip width (inches)
1	45.0	3.145	1.0	5.407	0.1330
2	45.0	3.145	1.0	5.540	0.1335
3	45.0	3.145	1.0	5.674	0.1335
4	45.0	3.145	1.0	5.807	0.1335
5	45.0	3.145	1.0	5.941	0.1335
6	45.0	3.145	1.0	6.074	0.1335
7	45.0	3.145	1.0	6.208	0.1335
8	45.0	3.145	1.0	6.341	0.1335
9	45.0	3.145	1.0	6.475	0.1335
10	45.0	3.145	1.0	6.608	0.0669

Table 2: Mode shapes and frequencies used in the study

Table 2.1: Mode 1: natural frequency=81.376 HZ

Strip Index	Bending	Torsion
1	0.0	0.328
2	0.0	0.444
3	0.0	0.584
4	0.0	0.627
5	0.0	0.693
6	0.0	0.742
7	0.0	0.793
8	0.0	0.889
9	0.0	0.937
10	0.0	1.000

Table 2.2: Mode 2: natural frequency=148.02 HZ

Strip Index	Bending	Torsion
1	-0.082	0.329
2	-0.087	0.446
3	-0.070	0.586
4	-0.058	0.630
5	-0.034	0.696
6	0.0	0.745
7	0.076	0.796
8	0.203	0.892
9	0.358	0.940
10	0.502	1.003

Table A.1

Mass and Stiffness matrices for a tuned cascade

Mass matrix		Stiffness matrix	
258.5	0.0	32.9456	0.0
0.0	86.1815	0.0	86.1815

Table A.2

Comparison of MISER and ASTROP2 calculations for a tuned cascade

Calculation Code	Aerodynamic matrix, A	Force matrix, G	Flutter frequency and damping	Response magnitude
ASTROP2	11 (-1.7174, -4.7294) 12 (-12.902,-2.6919) 21 (0.10711,-3.2800) 22 (-7.3775,-5.9327)	11 (-4.2854,7.4543) 21 (-3.5772,4.2408)	(0.35816,-0.00325) (1.04310,-0.04040)	0.02553 0.23416
MISER	11 (-1.7174, -4.7294) 12 (-12.902,-2.6919) 21 (0.10711,-3.2800) 22 (-7.3775,-5.9327)	11 (-4.2854,7.4543) 21 (-3.5772,4.2408)	(0.35816,-0.00325) (1.04310,-0.04040)	0.02553 0.23416

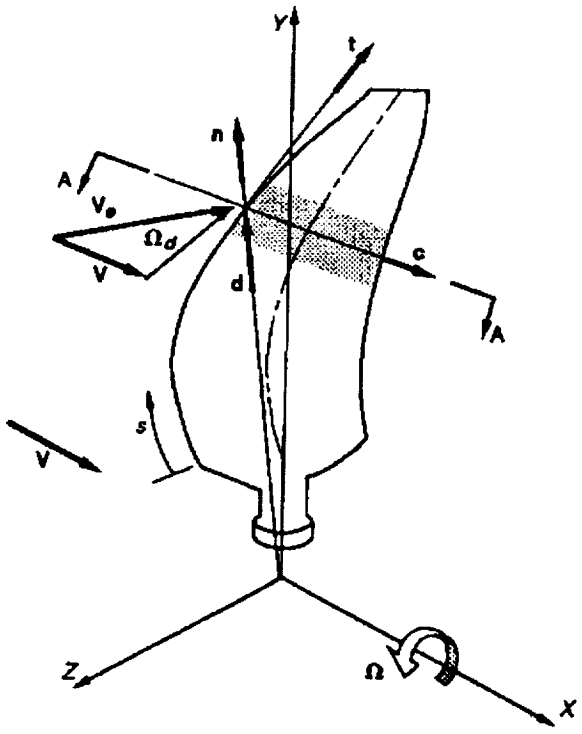

Figure 1a: ASTROP2 coordinate system for a rotating blade

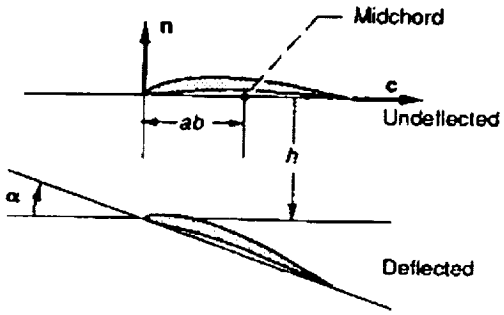

section A-A

Figure 1b: Section A-A showing rigid pitching (α) and plunging (h) motions for the strip (reference axis =leading edge)

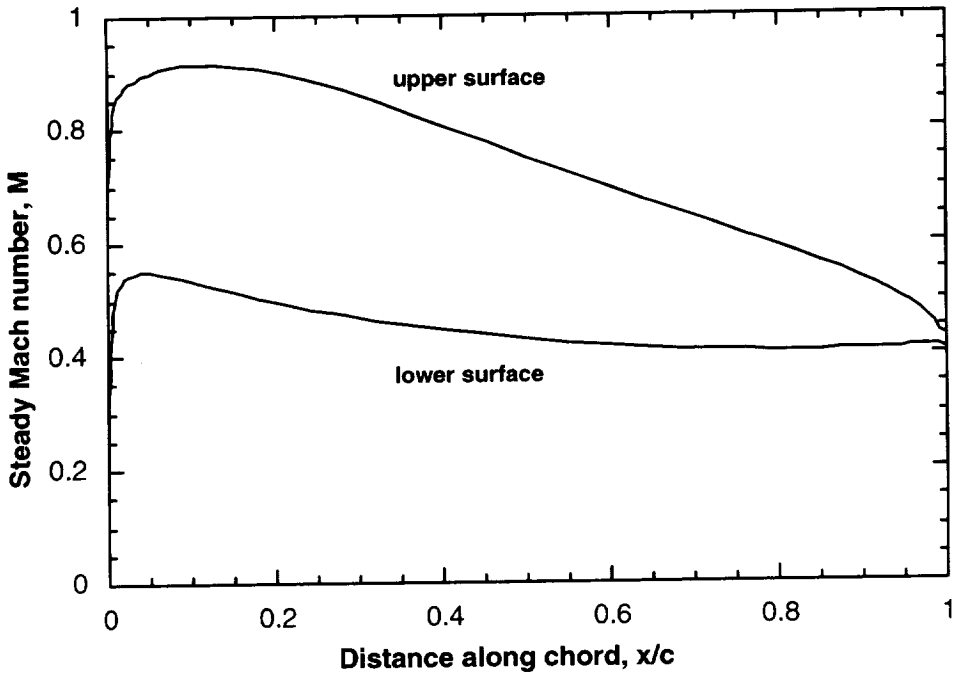

Figure 2a: Steady Mach number distribution for a subsonic cascade, C10 airfoil, gap to chord ratio, s/c=1.0, stagger angle, θ =45 degrees, inlet Mach number, M =0.7, angle of attack, i =10 degrees.

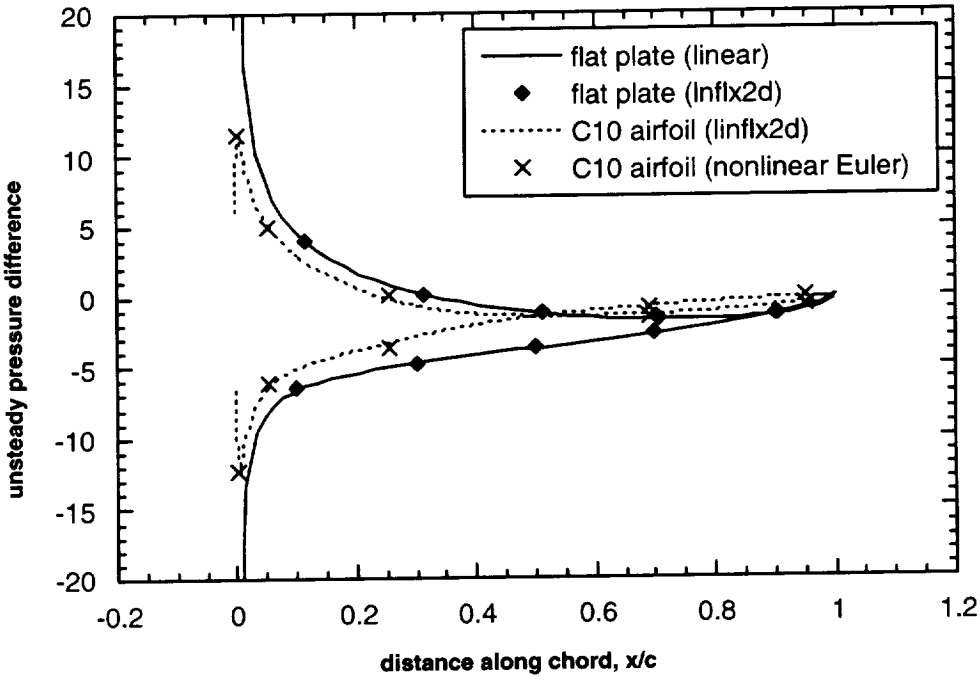

Figure 2b: Unsteady pressure difference distribution for a subsonic cascade, pitching about midchord, s/c=1.0, θ =45 deg., M=0.7, k_c=1.0, interblade phase angle, σ=180 deg., amplitude of oscillation, α_O =2 deg., i=0 degrees for flat plate and i=10 degrees for C10 airfoil

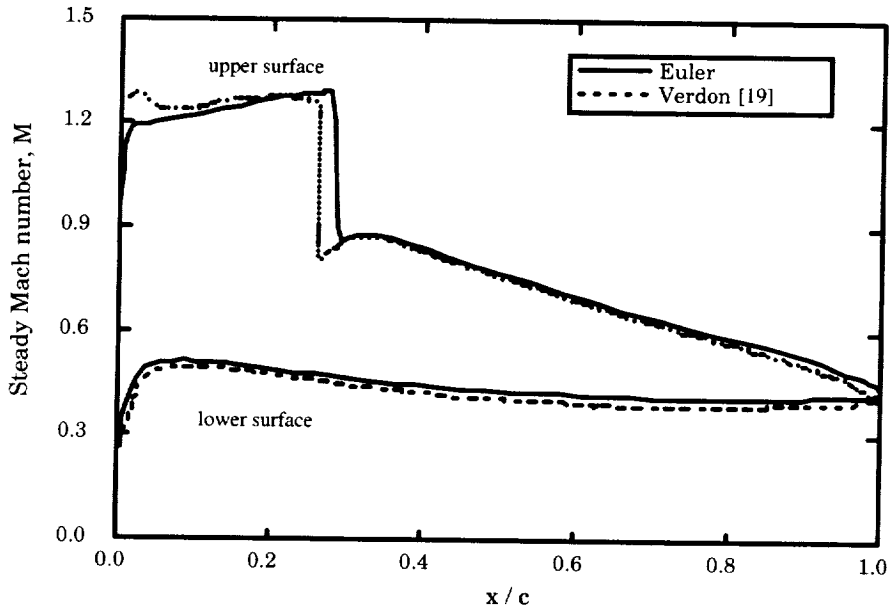

Figure 3a: Steady Mach number distribution for a transonic cascade; C10 configuration, $s/c = 1.0$, $\theta = 45°$, $M = 0.8$, $i = 13°$.

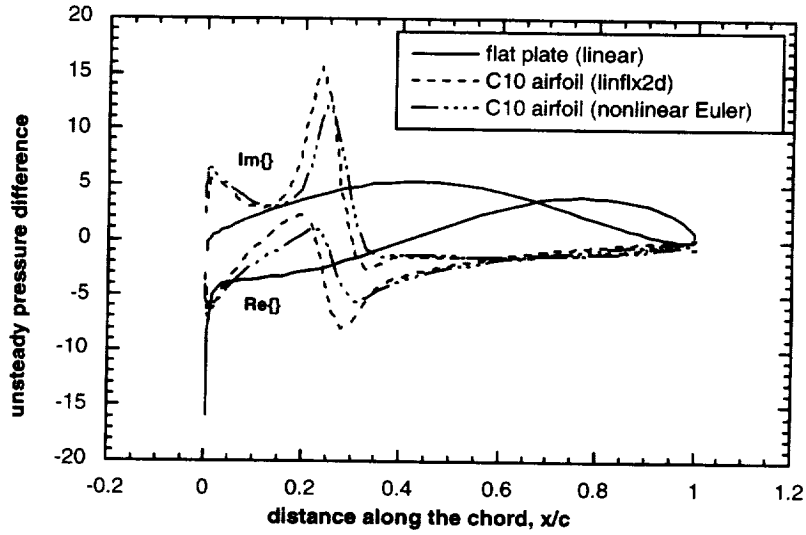

Figure 3b: Unsteady pressure difference distribution for a transonic cascade; C10 configuration, pitching about mid-chord; parameters as in Fig. 3a, $k_b = 0.5$, $\sigma = 180°$, $\alpha_o = 2°$.

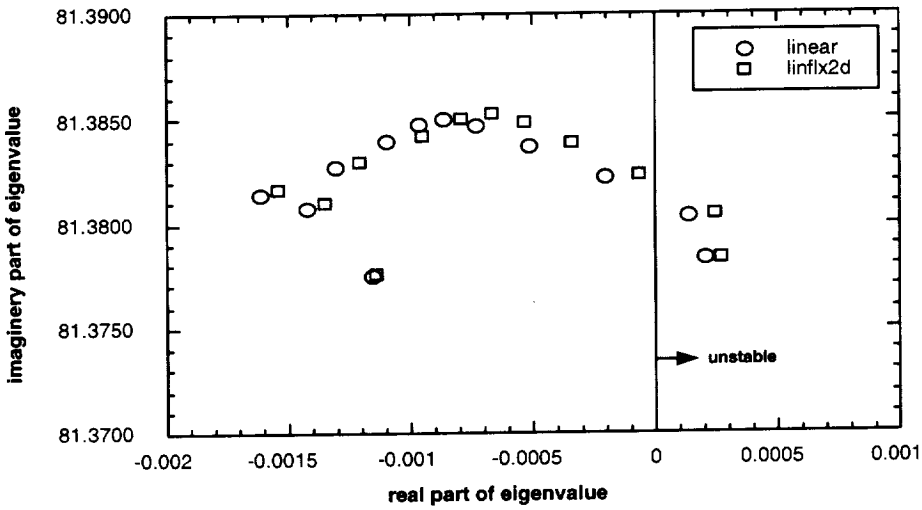

Figure 4: Root locus plot for 12 blade tuned cascade, first mode, flat plate geometry, $k_b = 0.1$, structural damping ratio = 0.0, M=0.7

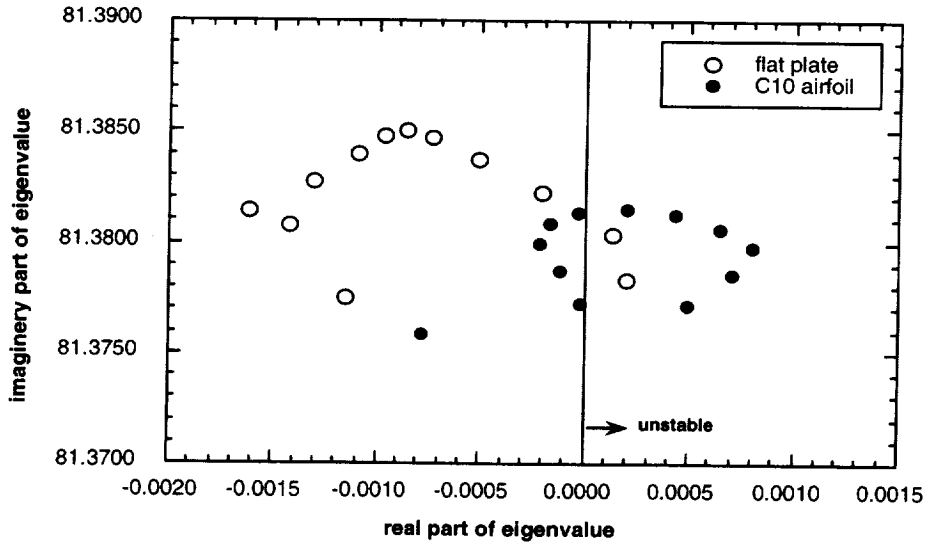

Figure 5a: Root locus plot for a 12 blade tuned cascade, first mode, flat plate and C10 geometries, k_b = 0.1, structural damping ratio =0.0, M=0.7

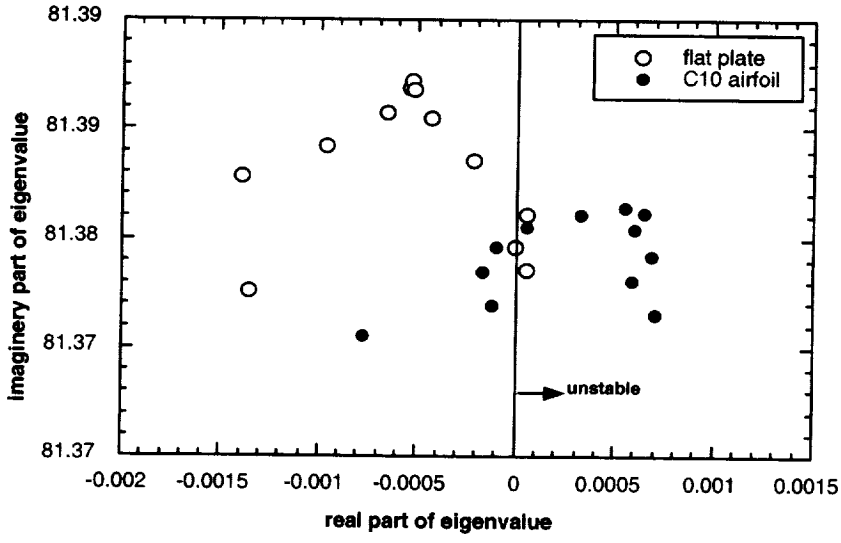

Figure 5b: Root locus plot for a12 blade tuned cascade, first mode, flat plate and C10 geometries, k_b = 0.1, structural damping ratio =0.0, M=0.8

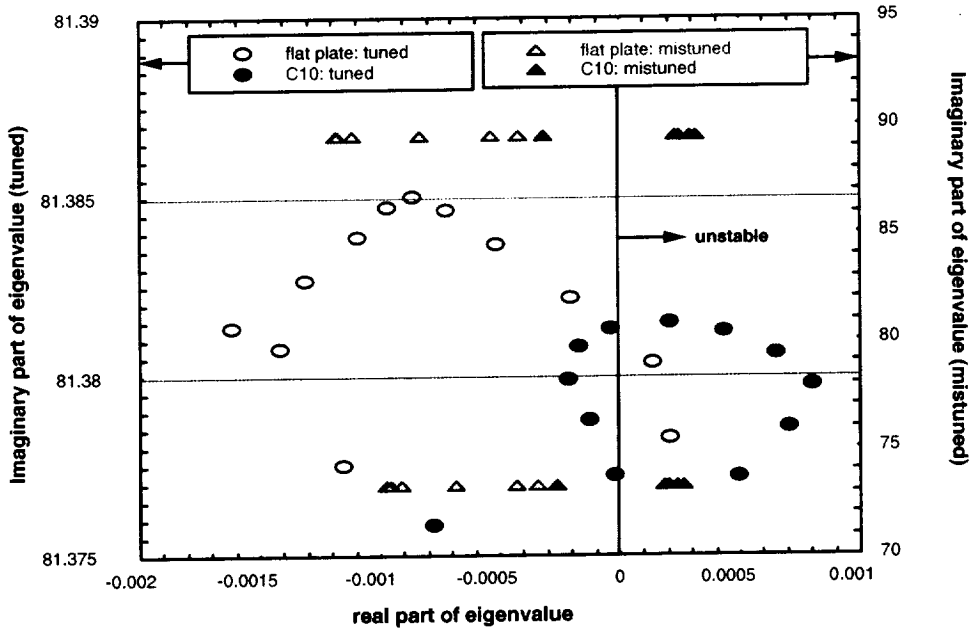

Figure 6a: Root locus plot for a12 blade mistuned cascade, first mode, 20% alternate mistuning; circles: tuned cascade; triangles: mistuned cascade; open symbol: flat plate; closed symbol: C10 airfoil, k_b = 0.1, structural damping ratio =0.0, M=0.7; note: left Y-axis refers to tuned cascade frequencies, and right Y-axis refers to mistuned cascade frequencies.

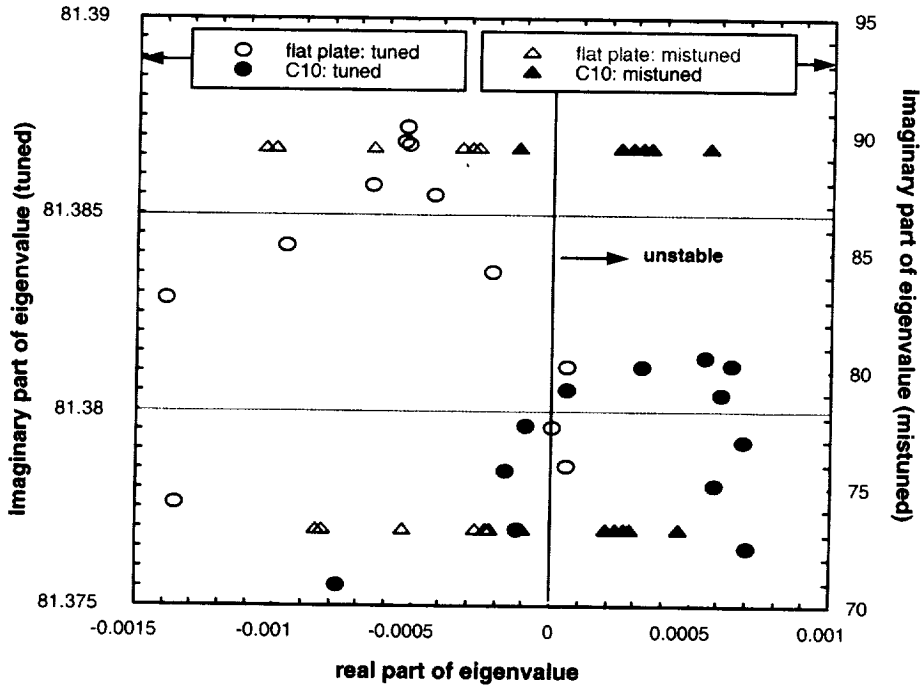

Figure 6b: Root locus plot for a12 blade mistuned cascade, first mode, 20% alternate mistuning; circles: tuned cascade; triangles: mistuned cascade; open symbol: flat plate; closed symbol: C10 airfoil, k_b = 0.1, structural damping ratio =0.0, M=0.8; note: left Y-axis refers to tuned cascade frequencies, and right Y-axis refers to mistuned cascade frequencies.

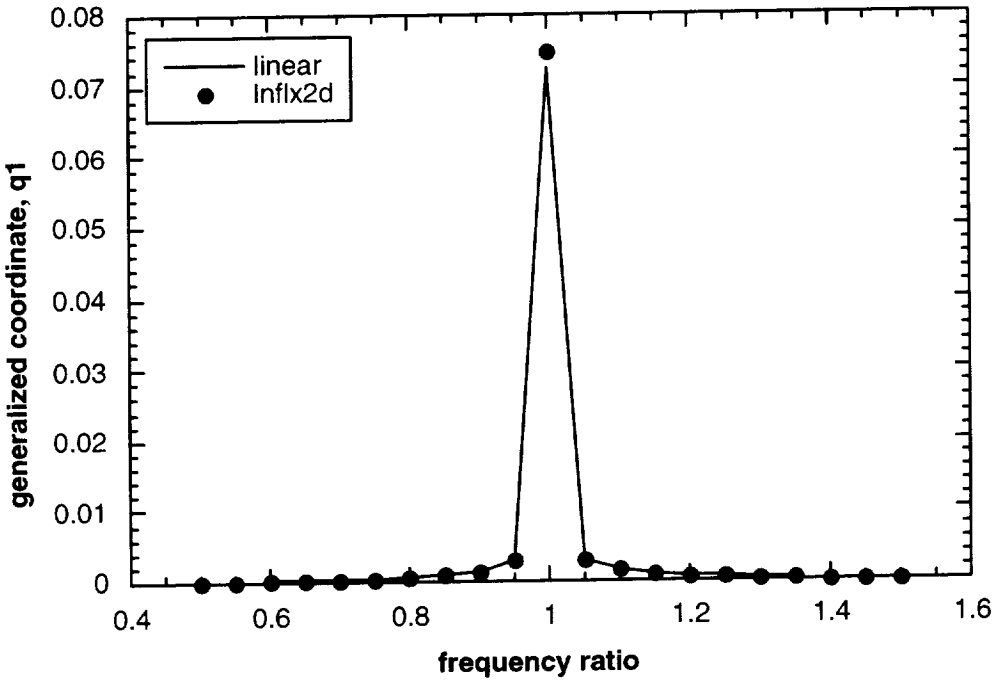

Figure 7: First mode response for a tuned cascade, flat plate geometry, structural damping =0.002, k_b = 0.1, N=12, flat plate geometry, M=0.7

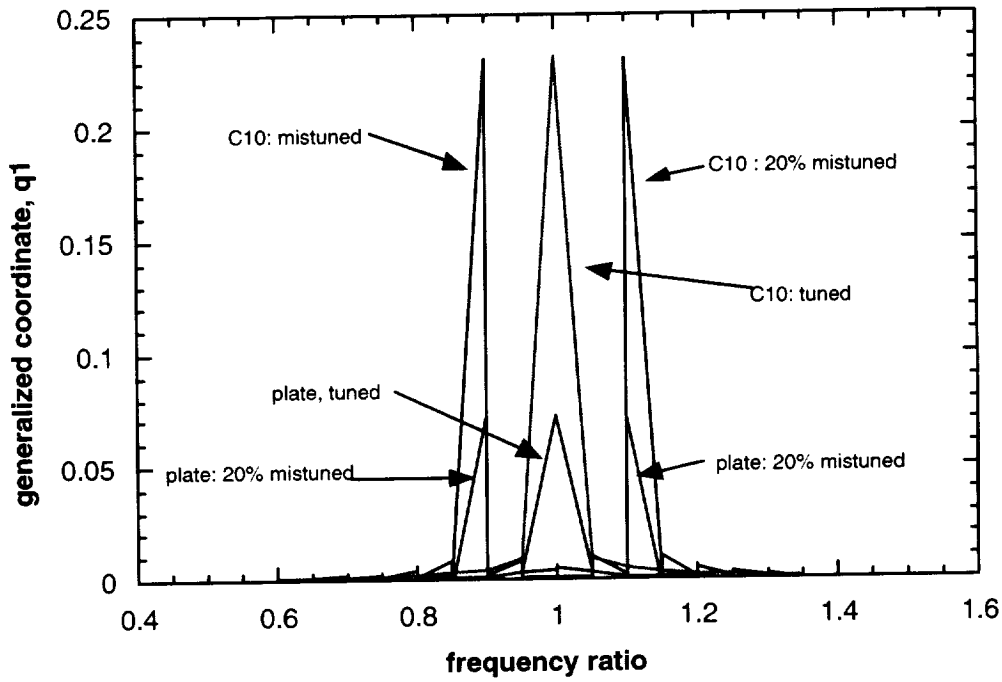

Figure 8: First mode response for a tuned cascade, flat plate geometry, structural damping ratio =0.002, k_b = 0.1, N=12, flat plate and C10 geometries, M=0.7

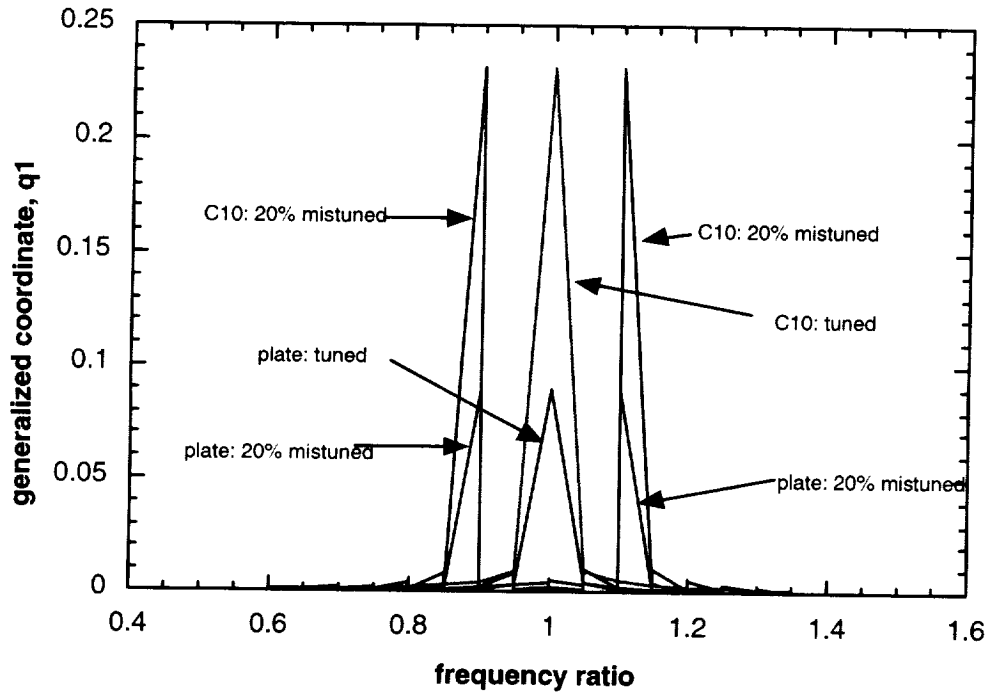

Figure 9: First mode response for a tuned cascade, flat plate geometry, structural damping =0.002, k_b = 0.1, N=12, flat plate and C10 geometries, M=0.8

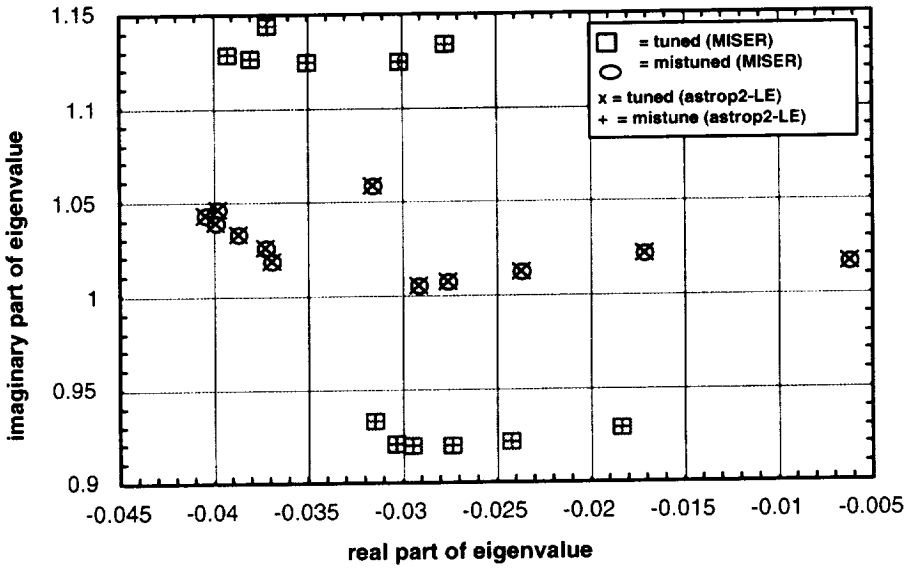

Figure A1. root locus plot for the second mode; 12 blades, s/c=1.0, stagger=45, Pitching about leading edge, kb=0.5, M=0.7, flat plate

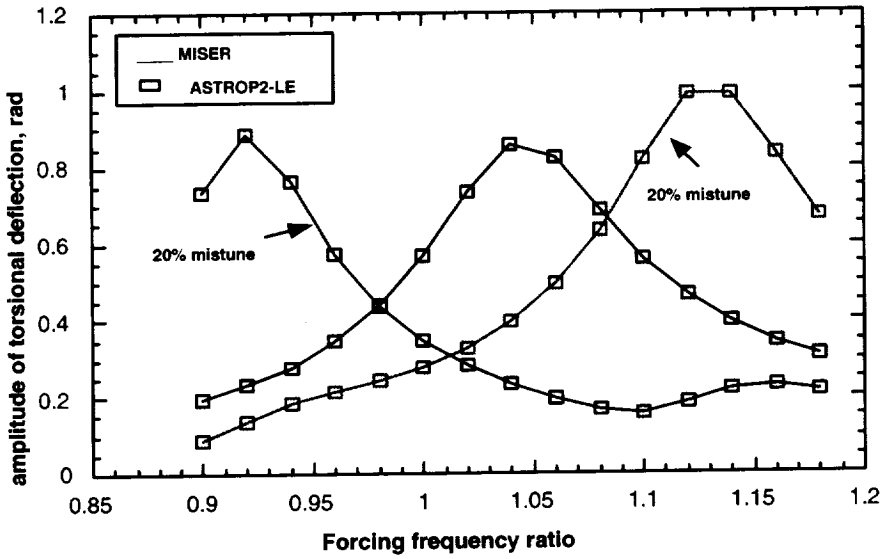

Figure A2. forced response, R=6(sigma=180 degrees)

REPORT DOCUMENTATION PAGE

Form Approved
OMB No. 0704-0188

1. AGENCY USE ONLY (Leave blank)	2. REPORT DATE	3. REPORT TYPE AND DATES COVERED
	May 2002	Technical Memorandum

4. TITLE AND SUBTITLE

ASTROP2-LE: A Mistuned Aeroelastic Analysis System Based on a Two Dimensional Linearized Euler Solver

5. FUNDING NUMBERS

WU-708-28-13-00

6. AUTHOR(S)

T.S.R. Reddy, R. Srivastava, and O. Mehmed

7. PERFORMING ORGANIZATION NAME(S) AND ADDRESS(ES)

National Aeronautics and Space Administration
John H. Glenn Research Center at Lewis Field
Cleveland, Ohio 44135-3191

8. PERFORMING ORGANIZATION REPORT NUMBER

E-13266

9. SPONSORING/MONITORING AGENCY NAME(S) AND ADDRESS(ES)

National Aeronautics and Space Administration
Washington, DC 20546-0001

10. SPONSORING/MONITORING AGENCY REPORT NUMBER

NASA TM—2002-211499

11. SUPPLEMENTARY NOTES

T.S.R. Reddy and R. Srivastava, University of Toledo, Toledo, Ohio 43606 and NASA Resident Research Associates at Glenn Research Center; and O. Mehmed, NASA Glenn Research Center. Responsible person, T.S.R. Reddy, organization code 5930, 216–433–6083.

12a. DISTRIBUTION/AVAILABILITY STATEMENT

Unclassified - Unlimited
Subject Category: 39 Distribution: Nonstandard

Available electronically at http://gltrs.grc.nasa.gov/GLTRS

This publication is available from the NASA Center for AeroSpace Information, 301–621–0390.

12b. DISTRIBUTION CODE

13. ABSTRACT (Maximum 200 words)

An aeroelastic analysis system for flutter and forced response analysis of turbomachines based on a two-dimensional linearized unsteady Euler solver has been developed. The ASTROP2 code, an aeroelastic stability analysis program for turbomachinery, was used as a basis for this development. The ASTROP2 code uses strip theory to couple a two dimensional aerodynamic model with a three dimensional structural model. The code was modified to include forced response capability. The formulation was also modified to include aeroelastic analysis with mistuning. A linearized unsteady Euler solver, LINFLX2D is added to model the unsteady aerodynamics in ASTROP2. By calculating the unsteady aerodynamic loads using LINFLX2D, it is possible to include the effects of transonic flow on flutter and forced response in the analysis. The stability is inferred from an eigenvalue analysis. The revised code, ASTROP2-LE for ASTROP2 code using Linearized Euler aerodynamics, is validated by comparing the predictions with those obtained using linear unsteady aerodynamic solutions.

14. SUBJECT TERMS	15. NUMBER OF PAGES
Flutter; Forced response; Cascades; Euler; Linearized; Mistuned	41
	16. PRICE CODE

17. SECURITY CLASSIFICATION OF REPORT	18. SECURITY CLASSIFICATION OF THIS PAGE	19. SECURITY CLASSIFICATION OF ABSTRACT	20. LIMITATION OF ABSTRACT
Unclassified	Unclassified	Unclassified	